energies

MDPI

Article

Beeswax–EVA/Activated-Charcoal-Based Fuels for Hybrid Rockets: Thermal and Ballistic Evaluation

Sri Nithya Mahottamananda [1], Yash Pal [2], Mengu Dinesh [3] and Antonella Ingenito [4,*]

[1] Department of Aerospace Engineering, B S Abdur Rahman Crescent Institute of Science & Technology, Chennai 600048, India
[2] School of Aeronautical Science, Hindustan Institute of Technology and Science, Chennai 603103, India
[3] Department of Aerospace Engineering, Karunya Institute of Technology and Sciences, Coimbatore 641114, India
[4] School of Aerospace Engineering, Sapienza University of Rome, 00138 Rome, Italy
* Correspondence: antonella.ingenito@uniroma1.it

Abstract: Beeswax ($C_{46}H_{92}O$) is a naturally derived substance that has the potential to be used as a solid fuel for hybrid rocket applications and as a substitute for paraffin wax fuel in hybrid rockets. BW burns more efficiently than paraffin wax because of the oxygen molecule it contains. The low thermal stability and poor mechanical properties of BW limit its practical use for upper-stage propulsion applications, and these issues are rarely addressed in the literature on hybrid rockets. This study investigates the thermal stability and ballistic properties of BW using ethylene-vinyl acetate (EVA) and activated charcoal (AC) as an additive. The thermal stability of BW–EVA/AC fuel compositions was analyzed using a thermogravimetric analyzer (TGA). The thermal stability of the blended BW compositions improved significantly. A laboratory-scale hybrid rocket motor was used to evaluate such aspects of ballistic performance as regression rate, characteristic velocity, and combustion efficiency. The results revealed that the pure BW exhibited a higher regression rate of 26.5% at an oxidizer mass flux of 96.4 kg/m^2-s compared to BW–EVA/AC blends. The addition of EVA and AC to BW was found to increase the experimental characteristic velocity and combustion efficiency. The combustion efficiency of BW-based fuel was improved from 62% to 94% when 20 wt.% EVA and 2 wt.% AC were added into the fuel matrix.

Keywords: beeswax; ethylene-vinyl acetate; activated charcoal; regression rate; combustion efficiency; hybrid rocket motor

Citation: Mahottamananda, S.N.; Pal, Y.; Dinesh, M.; Ingenito, A. Beeswax–EVA/Activated-Charcoal-Based Fuels for Hybrid Rockets: Thermal and Ballistic Evaluation. *Energies* **2022**, *15*, 7578. https://doi.org/10.3390/en15207578

Academic Editor: Devinder Mahajan

Received: 1 September 2022
Accepted: 10 October 2022
Published: 14 October 2022

1. Introduction

The hybrid propulsion system has emerged as a potential competitor to the conventional solid and liquid propulsion systems, as it has the advantages of both while providing a solution to their potential issues [1,2]. Unlike solid rockets, hybrid rockets offer safety, restart capability, and low operational costs. Additionally, hybrid rockets are less complex and have a higher density-specific impulse than liquid rockets [3–5]. Despite these benefits and significant research efforts over the past few years, hybrid rockets have not yet been used in practical applications. On the other hand, the low regression rate and low combustion efficiency are the main drawbacks that limit the maturity level of this technology [4,6]. The regression rate of hybrid fuel plays a significant role in developing a viable hybrid rocket propulsion system. The accurate prediction of the regression rate can also help designers develop main components and subassemblies, including the injector system and combustion chamber. The low regression rate of solid fuel in hybrid rockets leads to low thrust-to-weight ratios compared to successful solid rockets. Several techniques have been reported to enhance the regression rate performance of solid fuel, including the addition of metal and metal hydrides [7–11] and the use of multi-port fuel grains [12,13], mixed hybrid fuels [14,15], wax-based fuels [16], the swirl injection method [17–19], protrusions [20–25], bluff-bodies [26], and cavities [27].

Karabeyoglu et al. [16] proposed paraffin wax as a potential alternative to conventional polymer-based fuels such as hydroxyl-terminated polybutadiene (HTPB), polyethylene (PE), and polymethyl methacrylate (PMMA). Regression rates of paraffin waxes are 3 to 5 times higher than those of conventional fuels [16]. These findings brought a paradigm shift in hybrid rocket research and developmental activities in academia and industries. Paraffin wax is easily available, low cost, environmentally friendly, and has the quickest process time and least infrastructure required to manufacture the fuel grains. The higher regression rate characteristics of wax-based fuels are attributed to their droplet entrainment phenomenon during combustion [16,21]. The combustion process of the paraffin wax fuel in the hybrid rocket is illustrated in Figure 1. It can be observed that a melt layer with finite thickness develops over the fuel surface during the combustion process. The melt layer periodically gets sheared off due to the high injection velocities of the oxidizer; as a result, instability occurs within the melt layer, forming a wave-like structure. Due to this, the melted wax entrains in the form of droplets. These droplets diffuse into the oxidizer-rich region beyond the flame zone and participate in the combustion process. Droplets can eventually burn up within the boundary layer depending on the oxygen concentration.

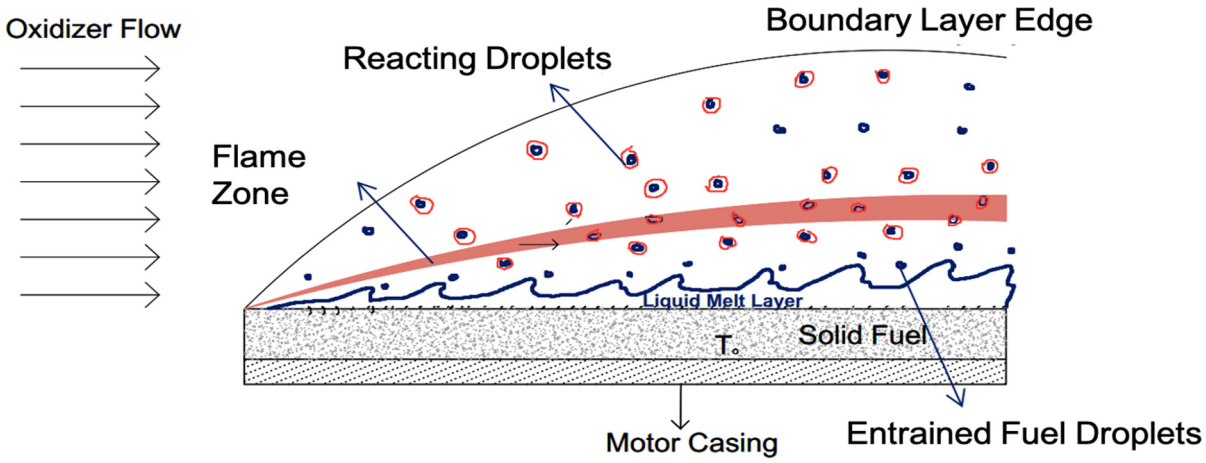

Figure 1. The combustion process of paraffin wax-based fuels in hybrid rockets.

The entrained wax droplets require sufficient residence time to combust within the chamber completely. Due to diffusion-limited combustion, the droplets exit the nozzle without fully combusting, leading to lower combustion efficiency of the hybrid rocket motors. When being stored, handled, or used, paraffin wax might deform due to its low melting temperature range (50–65 °C). Sometimes, slump deformation could have the potential for longer storage life where temperatures exceed 45 °C. Therefore, one of the essential requirements for practical hybrid applications is enhancing the wax's mechanical and thermal stability. Various strengthening additives have been used to enhance the thermal stability of paraffin wax [6,28,29]. In some cases, blending HTPB with paraffin wax improved the mechanical and thermal stability of fuel formulations [5,6,29,30]. To understand the wax's thermal stability when polymeric additives are added, several investigations into the thermal degradation of wax have been carried out [6,28,29,31]. It was found that the addition of polymeric additives enhanced the melting point of paraffin wax.

The regression rate of paraffin-based fuels decreases with the addition of strengthening additives [32–36]. This has been attributed to the increased melt-layer viscosity of the wax when polymers are added. Since viscosity is inversely related to entrainment mass flow rate, the overall regression rate decreases with an increase in viscosity [37,38]. Therefore, the mechanical properties and thermal stability of wax can be improved by adding strengthening additives at the cost of regression rate [39]. In contrast, the combustion efficiency improved by adding polymeric additives to wax [2,33,40] due to the wax evaporation from the melted layer instead of entrainment mass transfer. According to earlier experiments, adding 3% carbon black to paraffin wax fuels improved the regression

rate by up to 30% [41]. As carbon black increases the opacity of wax fuel, it improves the radiant heat transfer over the solid fuel surface. Activated charcoal (AC) was used as a burn-rate enhancer in the composite solid propellant and can serve as an effective additive to enhance the regression rate of solid fuel. Due to the porous nature of activated charcoal, it promotes oxygen diffusion to the particles, potentially enabling rapid ignition and burning of charcoal particles [41–43]. The rapid ignition may also augment the combustion of metal particles by increasing the local temperature. The addition of AC to composite solid propellants showed significant burn rate improvement and suppressed the pressure index [43]. However, the effectiveness of AC with wax-based fuels for hybrid rocket applications has not explicitly been investigated.

Similar to paraffin wax, BW can be used as a solid fuel in hybrid rockets [44–46]. The extra oxygen atom in BW could promote an oxidation reaction within the boundary-layer flame structure and enhance the overall combustion. Jayapal et al. [29] reported that the activation energy of BW–EV fuel was reduced with the addition of AC. Previous research has demonstrated that the regression rates of BW and paraffin wax are comparable [47,48]. Putnam [44] performed experiments with BW–nitrous oxide hybrid rockets. A 1% improvement in specific impulse was shown via theoretical analysis of BW burning with gaseous oxygen at 20% aluminum loading. According to the experimental findings, BW–oxygen consistently had a comparable regression rate to paraffin wax. Naoumov et al. [48] developed regression rates data for beeswax and paraffin wax with 10% micro-aluminum loading in each fuel through a series of hot-fire tests. The results showed a marginal improvement in the regression rate with the addition of aluminum. However, the regression rate of BW fuels was consistently above that of paraffin wax fuels. Recently, Stober et al. [47] studied the feasibility of BW as an alternative to paraffin wax for orbit propulsion applications. In this study, the centrifugal casting method was used to manufacture the BW- and paraffin wax-based fuel grains for in-space small satellite propulsion applications. Mahottamananda et al. [29,49,50] performed a series of thermal and mechanical characterization tests for beeswax mixed with EVA, HTPB, and AC. However, the regression rate characteristics were not studied by this group.

Although BW and paraffin wax have different physical properties, it was found from the literature that both waxes have poor mechanical properties. As a result, wax fuels are unlikely to be used for practical hybrid rocket applications. BW has not received much attention in previous studies, which have largely focused on enhancing the mechanical properties of paraffin and microcrystalline wax [32–34]. In the past, authors [50] have attempted to improve the mechanical properties of BW by using EVA as an additive. Although the EVA improved the mechanical properties, its effect on the regression rate was not evaluated. Therefore, it is important to understand the effect of polymeric additives on the regression rate of the BW as it exhibits a different molecular structure to paraffin wax. Furthermore, it was discovered that the thermal and mechanical properties of wax can be enhanced at the expense of the regression rate. Finding the ideal balance between the mechanical, thermal, and ballistic qualities is always important to produce a good quality of wax-based fuel for upper-stage applications. Further investigation is required to fully understand the ballistic properties of wax-polymer fuels with AC. This study can also be used to understand how metal particles in wax-polymer fuels behave during combustion because AC can raise the local temperature through quick ignition. Based on the preceding discussion, efforts have been made recently to examine the thermal and ballistic characteristics of BW fuel blended with EVA and AC. Thermogravimetric analysis (TGA) was used to understand the thermal stability of the fuel compositions. Surface morphological studies have also been conducted to observe the network of EVA and AC in the BW using a scanning electron microscope (SEM). A laboratory-scale hybrid rocket motor was used to evaluate the ballistic characteristics, including regression rate and combustion efficiency.

2. Experimental Setup

2.1. Materials and Fuel Grain Preparation

In the present study, BW was used as the fuel, and EVA and activated charcoal (AC) were used as additives for improving the mechanical and ballistic properties, respectively. The details of the chemicals procured for this study are given in Table 1.

Table 1. Chemicals used for hybrid fuel preparation.

Chemical	Chemical Formula	Density, kg/m^3	Supplier
Beeswax (BW)	$C_{46}H_{92}O$	970	Unicorn Petroleum Industries Private Limited, Mumbai
Ethylene-vinyl acetate (EVA)	$(C_2H_4)_4(C_4H_6)_2$	950	Happy Plastics, Mumbai
Activated charcoal (AC)	C	1480	Sigma Aldrich

Table 2 displays five different types of BW fuel sample composition used in the present study. The EVA percentage in BW varied between 10% and 20%, and the AC varied between 1% and 2%.

Table 2. Compositions of BW–EVA-based solid fuels.

Sample	Composition	Beeswax (wt.%)	EVA (wt.%)	Activated Charcoal (wt.%)
B1	100% BW	100	-	-
B2	90% BW + 10% EVA	90	10	-
B3	80% BW + 20% EVA	80	20	-
B4	89% BW + 10% EVA + 1% AC	89	10	1
B5	78% BW + 20% EVA + 2% AC	78	20	2

The solid fuel grains were prepared using a typical melt-cast method. The required quantities of beeswax and EVA were melted in a heating bowl, followed by mechanical stirring to ensure uniform mixing. The activated charcoal was added to the blend of EVA and BW and stirred for 20 min. The melted fuel was then poured into the mold and allowed to solidify at room temperature for 6 h. The prepared solid fuel grains are shown in Figure 2.

Figure 2. Beeswax–EVA-based solid fuel grains after solidification.

2.2. Thermogravimetric and Scanning Electron Microscope Analysis

The thermal stability of the Beeswax-EVA/AC-based solid fuel samples was analyzed using a simultaneous thermal analyzer (TGA-DSC) (Model: NETZSCH STA 449F3 Jupiter apparatus) in a nitrogen atmosphere. The measurement was carried out at a constant

nitrogen flow rate of 20 mL min^{-1} and a heating rate of 10 °C/min. Furthermore, the surface morphology of BW–EVA/AC blends was analyzed using high-resolution scanning electron microscopy (Model: JEOL Japan, JEM-2100 Plus). Fuel samples were coated with gold to prevent overcharging and provide conductivity in the sample.

2.3. Hybrid Rocket Motor

The hybrid rocket motor used for the ballistic evaluation was fabricated using stainless steel, and a schematic view is shown in Figure 3. The hybrid rocket motor consists of an injector plate, combustion chamber, and a CD nozzle. In the current study, gaseous oxygen was supplied using an axial injection technique. The inner and outer diameters of the combustion chamber were 80 and 90 mm, respectively. The convergent–divergent nozzle made of graphite was used with a nozzle inlet and throat diameter of 80 and 14.3 mm, respectively. The nozzle was fabricated with a 45° converging angle and diverging angle of 15°. The initial port diameter of the fuel grain was 30 mm.

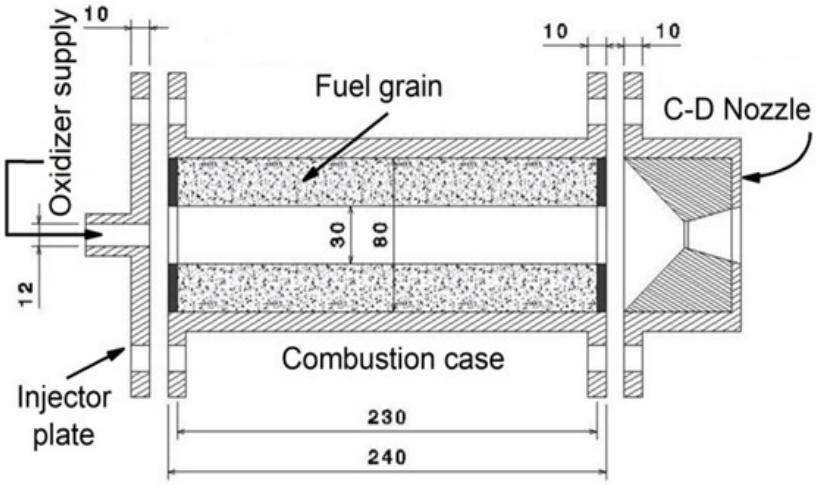

Figure 3. Schematic diagram of hybrid rocket motor (all dimensions in mm).

2.4. Ballistic Test Facility and Operating Procedure

The schematic layout of the hybrid rocket motor ballistic test facility is presented in Figure 4. The experimental facility consists of an oxidizer feed system, oxidizer control unit, ignition system, and lab-scale hybrid rocket motor. The pressure regulator was used to set the injection pressure, and the solenoid valve was used to control the oxidizer flow. The solenoid valve and pyro-technique igniter were connected with a sequential timer (Model No.: PT-380), which helps to control the solenoid valve and igniter sequentially for the set time. A GE Druck UNIK5000 Series model piezo-resistive pressure transducer was used to measure the combustion chamber pressure. The data from the pressure sensors were acquired through the NI-9237 DAQ modules and LABVIEW software. The mass flow rate of the oxidizer was determined by measuring the weight of the oxygen cylinder before and after the combustion for a given time interval. The testing was carried out at a burn time of 5 s. The motor was mounted on the test bed, and ignition was initiated with the help of a rheostat arrangement connected to the sequential timer. As soon as ignition was achieved, the solenoid valve was opened, which was controlled by the sequential timer for a predetermined burn time. This solenoid valve allowed the gaseous-oxygen supply into the combustion chamber and initiated the combustion process. The high-pressure regulator controlled the oxygen injection pressure. When the set burn time was achieved, the sequential timer stopped the electric supply to the solenoid valve and cut off the oxygen flow into the chamber, which terminated the combustion process. The photographs of the hybrid motor mounted on the test bed, and test firing, are presented in Figure 5.

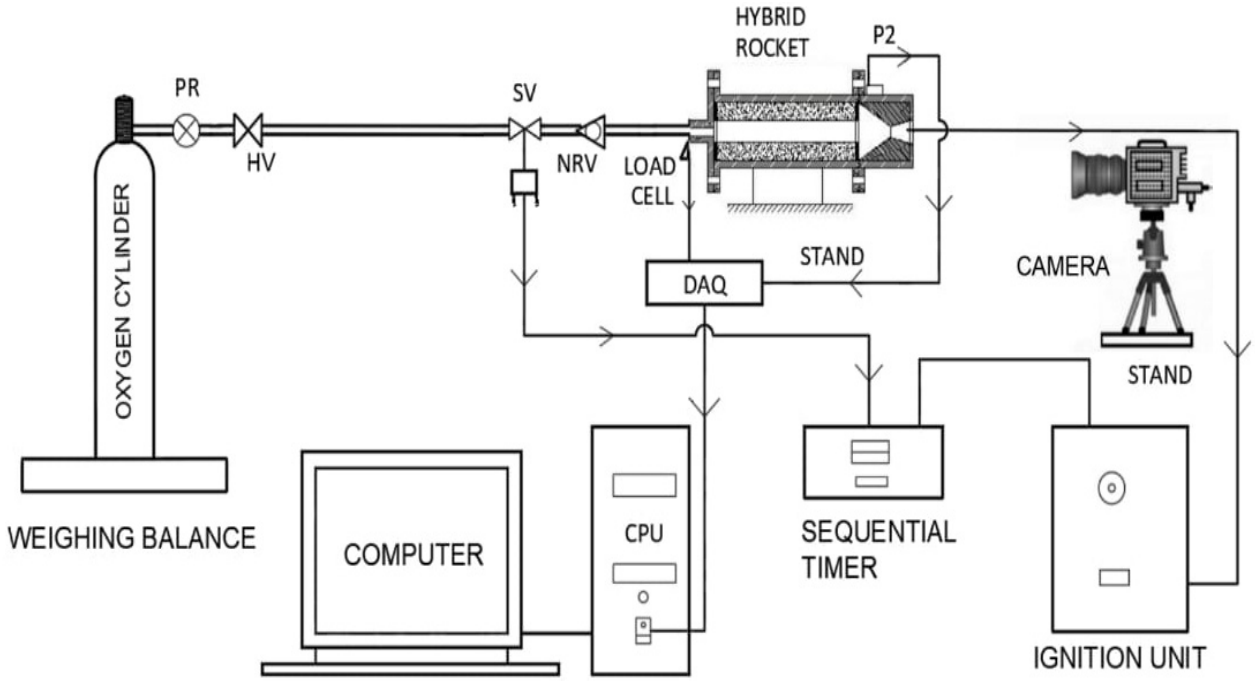

Figure 4. Schematic diagram of the oxygen feed line set up for the ballistic test.

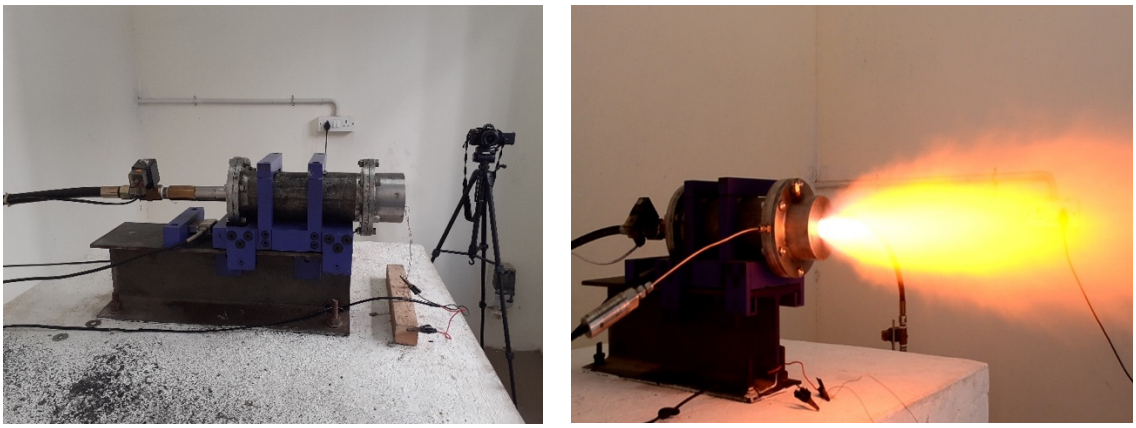

(**a**) (**b**)

Figure 5. Photographs of (**a**) hybrid rocket mounted on the thrust stand and (**b**) motor during the ballistic test.

2.5. Data Reduction Methodology

i. Regression Rate Measurement

In hybrid rockets, the fuel regression rate is defined as the rate at which the solid fuel is removed from the fuel surface. The pyrolysis process guides the fuel vapor into the combustion chamber when polymeric fuel is used, whereas the entrainment process controls the evaporation of wax into the combustion zone. The weight-loss method is the most commonly used technique to calculate the regression rate of solid fuel [51,52]. In the weight-loss method, the motor's weight is measured before and after the combustion for a given burn time (T_b). With the known fuel mass loss (m_b), the final fuel diameter (d_f) can be estimated using Equation (1), where ρ_f is the fuel density and l_f is the length of

the fuel grain. With the help of known d_f, d_i, and the burn time, the regression rate can be determined using Equation (2):

$$d_f = \sqrt{d_i^2 + \frac{m_b}{\frac{\pi}{4}\rho_f l_f}} \quad (1)$$

$$\dot{r} = \frac{d_f - d_i}{T_b} \quad (2)$$

The oxidizer mass flux (G_{ox}) was calculated using Equation (3), where $\dot{m}_{ox}$ is the oxygen mass flow rate and A_p is the average port area, which was calculated using Equation (4). The experiments were conducted for the different port diameters by maintaining the constant oxidizer mass flow rates.

$$G_{ox} = \frac{\dot{m}_{ox}}{A_p} \quad (3)$$

$$A_p = \frac{\pi}{4}\left(\frac{d_f + d_i}{2}\right)^2 \quad (4)$$

ii. Combustion efficiency

The present study estimated the combustion efficiency based on characteristic velocity. The combustion efficiency is determined using Equation (5), where c^*_{exp} is the experimental characteristic velocity and c^*_{theo} is the theoretical characteristic velocity. The experimental characteristic velocity can be calculated using Equation (6).

$$\eta^*_c = \frac{c^*_{exp}}{c^*_{theo}} \quad (5)$$

$$c^*_{exp} = \frac{A^* \int_0^{T_b} P_c \, dt}{\int_0^{T_b} \dot{m} dt + \Delta m_f} \quad (6)$$

The theoretical characteristic velocity was obtained through the code of NASA chemical equilibrium applications (NASA-SP 273) [53].

iii. Viscosity Measurement

The viscosity of the melt layer is known to increase when polymeric additives are added to wax fuels. As the melt layer viscosity directly influences the regression rate [34], it is vital to determine the viscosity of newly prepared fuel compositions. The viscosity of all fuel formulations was measured using a Brookfield DV-E viscometer. Low viscosity spindles are used to measure the viscosity. The experiments were performed at 90 °C and a strain rate of 22 S^{-1}. A hot-water bath was used to circulate the water around the fuel sample holder and keep the melted wax temperature constant.

3. Results and Discussion

3.1. Surface Morphology of BW–EVA/AC-Based Samples

Figure 6 shows the variation in surface morphology of the pure BW and its blended samples. It can be observed that the pure BW surface has a nodule-like structure, whereas a flake-like structure network can be observed in an 80%BW + 20%EVA composition (Figure 6b). The EVA is not completely miscible with beeswax. This is expected, as both have different molecular weights; the EVA network in BW acts like filler material and supports the wax mechanically under various load conditions. Similar structures have been observed in the literature when the wax is mixed with polyethylene (PE) [33] and low-density polyethylene (LDPE) [30]. In the case of 78%BW + 20%EVA + 2%AC fuel, the intensity of the flake-like structure increased, as shown in Figure 6c. This can be attributed to the deposition of the AC clusters in the BW–EVA blend. Hashim et al. [42] observed a similar clustering behavior in the HTPB fuel matrix containing boron and AC.

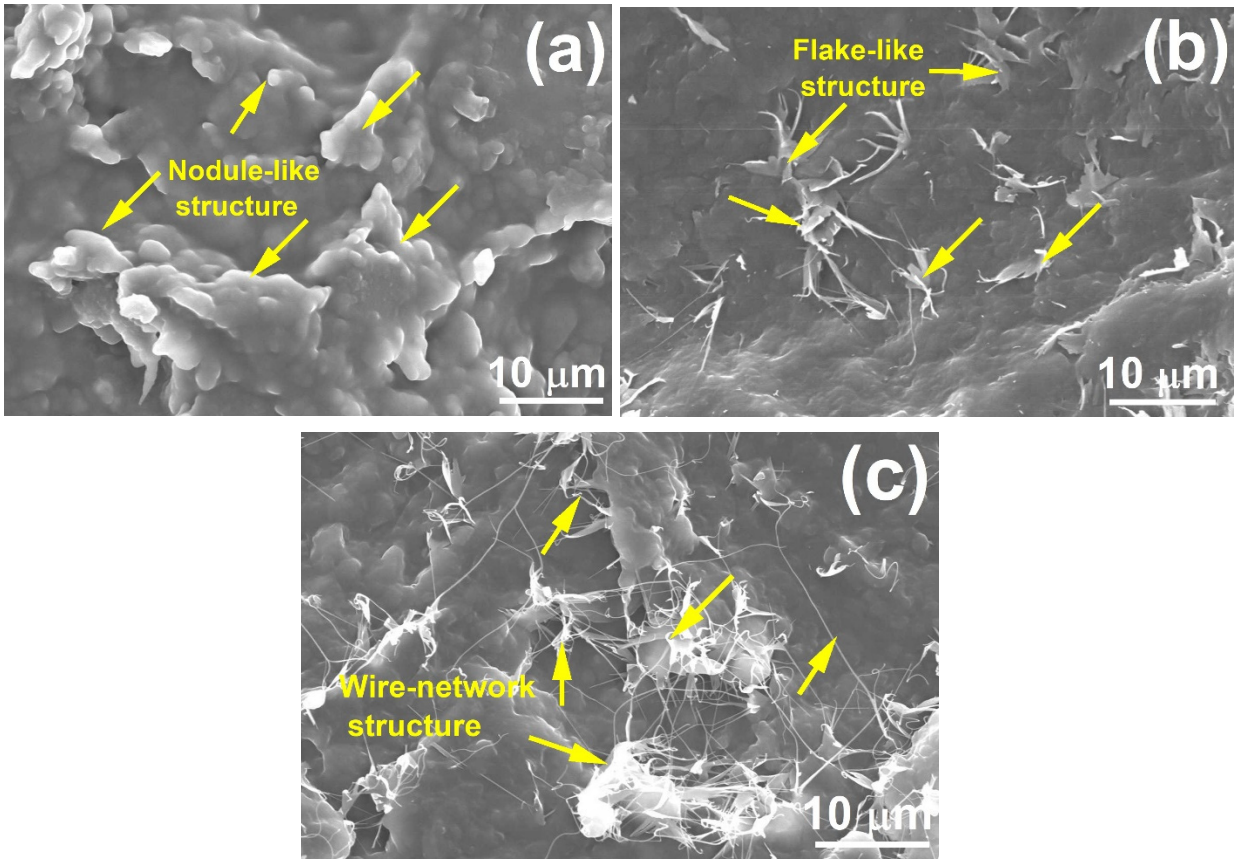

Figure 6. SEM morphology of beeswax-based fuel. (**a**) B1; (**b**) B3; (**c**) B5.

3.2. Thermal Stability of BW–EVA Based Solid Fuel Samples

The TGA experiments were performed in a nitrogen atmosphere at a heating rate of 10 °C/min in a temperature range of 25–650 °C. Figure 7 represents the TG curves of BW–EVA/AC fuel compositions. For pure BW, it can be observed that the onset temperature for the decomposition is 205.8 °C. The beeswax decomposed in a single step with 95% of the mass loss at the end of 451 °C heating. Based on the TGA plots from the literature, pure paraffin wax can be completely consumed at a temperature of around 330–350 °C [6,28,30]. At the same time, the decomposition temperature of BW is higher than that of paraffin wax [54]. Therefore, it can be said that the thermal stability of BW is higher than that of paraffin wax.

The thermal stability of all the fuel samples remained unchanged up to a temperature of 180 °C. The thermal stability of the BW improved with the addition of 20 wt.% of EVA. The onset temperature of the decompositions was increased from 205.8 °C to 227.3 °C. In the blended BW/EVA sample, the decomposition process occurred in two different stages. The first stage corresponds to wax decomposition (230–472 °C), and EVA started to degrade at 472 °C, (Figure 7). This kind of trend has also been confirmed in the literature [30], where wax mixed with LDPE at 10%. In the second stage, with the addition of 2 wt.% of AC to the BW/EVA sample, the thermal stability reduced with a marginal difference. This indicates that the presence of AC improved the decomposition process of wax and EVA. Furthermore, it was reported that the activation energy of wax-EVA fuel samples was reduced with the addition of AC [29]. Therefore, it is expected that adding AC would make the solid fuel pyrolysis faster, hence improving the regression rate.

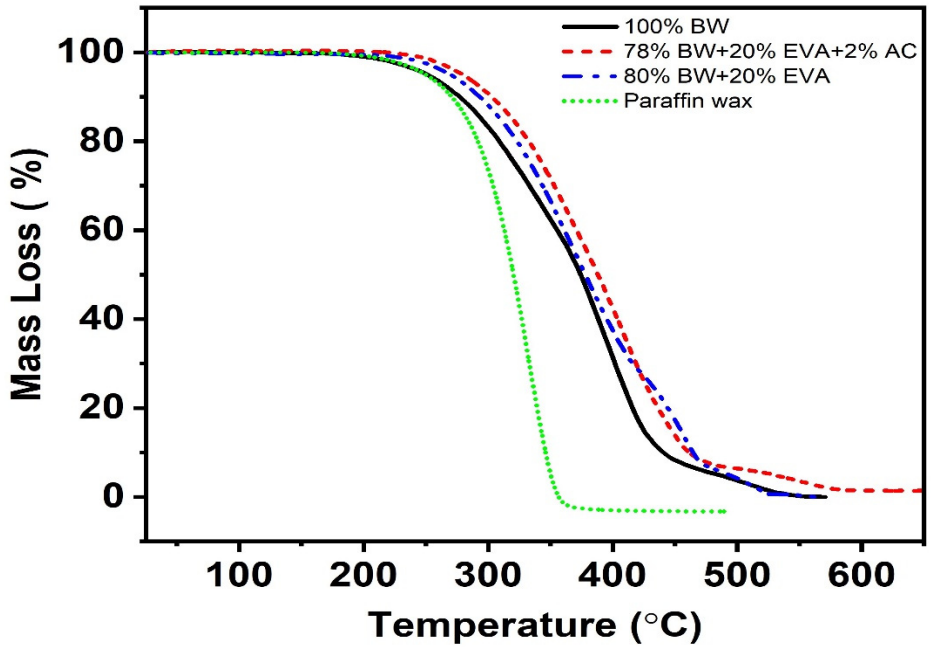

Figure 7. TG curves of BW–EVA-based solid fuels.

3.3. Regression Rate

Regression rate is an essential parameter in designing a hybrid rocket motor. Figure 8 shows the average regression rate versus oxidizer mass flux of the BW–EVA/AC fuel compositions. Furthermore, the ballistic test data are summarized in Table 3. It can be seen in Figure 8 that the pure BW exhibited the highest regression rate compared to the BW–EVA/AC fuel compositions. The higher regression rate characteristic is attributed to the entrainment of the fuel droplets from the melt layer during combustion. The fuel droplets are entrained by the shear force exerted by high injection velocity oxidizers, which is illustrated in Figure 1. The entrainment process strongly depends on the viscosity of the melt layer that forms on the solid fuel surface, i.e., the regression rate is inversely proportional to the viscosity of the melt layer [32,38]. When a polymeric additive such as EVA in the present study is added to wax, the viscosity of the melt layer tends to increase at a given temperature. A similar phenomenon has been observed for paraffin wax with polymeric additives [32,33,36,40,55,56]. As a result, Figure 8 and Table 3 show that adding EVA to BW reduced the regression rate. The regression rate is significantly reduced when 20% additional EVA is added to the wax. Additionally, to support the abovementioned facts, the viscosity of the fuel compositions was measured, and the results are listed in Table 4. The viscosity of the fuel samples was measured at 90 °C with a strain rate of 22 s^{-1}. Like the EVA wt.% increase in BW, the viscosity increased. Table 4 shows the results of the regression rate variation compared with the viscosity of BW-based fuel. The regression rate reduction increases as the EVA loading increases in BW both with AC and without AC.

Additionally, an attempt has been made to investigate how AC affects the regression rate of the BW–EVA blends. The BW–EVA blends were doped with 1 and 2 wt.% of AC. Adding AC to BW–EVA fuels increased the regression rate, as shown in Figure 8. At an oxidizer mass flux of 95 kg/m^2-s, the regression rate of the B4 (89% BW + 10% EVA + 1% AC) fuel sample increased by 13.88%, whereas a 5% improvement was observed with the B5 fuel sample. One can observe that adding a lower wt.% of AC to the BW–EVA blend would be more beneficial in improving the regression rate performance. According to Dinesh et al. [21,56], the higher viscosity of the melt layer prevents the entrainment of fuel droplets from the melt layer; instead, wax fuel undergoes pyrolysis to produce a significant amount of fuel vapor, which then ignites with oxygen. It is known that AC improves the radiative heat transfer to the fuel surface via its ignition; however, due to its lower thermal conductivity, rates of heat transfer to the adjacent layers of fuel may be reduced [42]. When

the AC loading in BW–EVA was increased, the AC displayed a high viscosity and reduced fuel pyrolysis rate due to its lower thermal conductivity. Hence, the regression rate is observed to be reduced with higher loading of AC in BW–EVA compositions. To reach a definite conclusion, however, additional trade-off studies on the regression rate of the BW–EVA/AC composite system are needed.

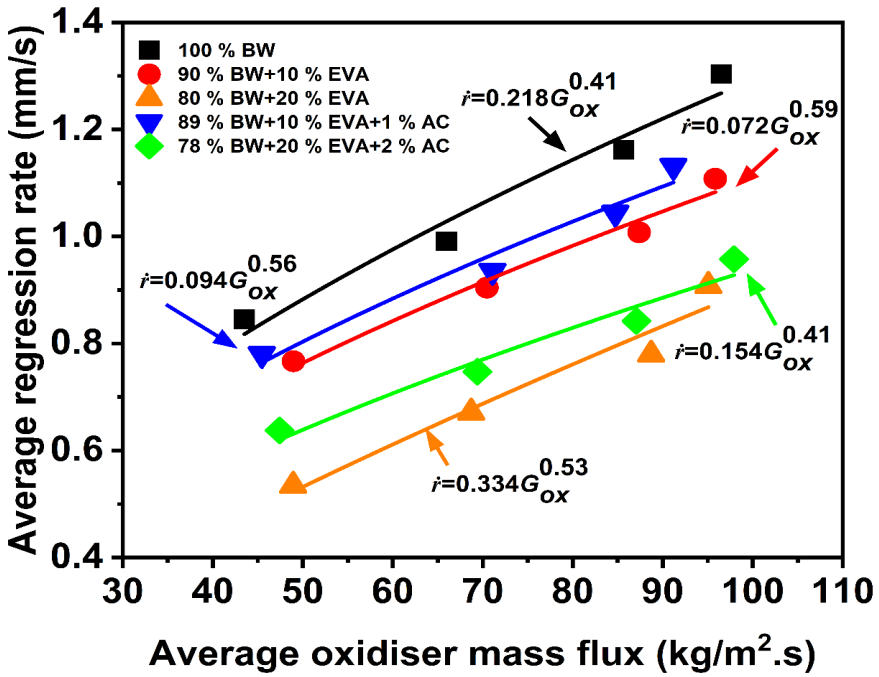

Figure 8. Average regression rate vs. oxidizer mass flux for prepared fuel grains. (Average regression rate uncertainty range: 1.2–3.5%.)

Table 3. Ballistic test data for BW–EVA-based solid fuels.

Fuel Sample	Chamber Pressure (MPa)	Mass of Fuel Consumed (kg)	Oxidizer Mass Flux G_{ox}, (kg/m^2-s) *	Regression Rate (mm/s)	Regression Rate Exponents	
					a	*n* #
100% BW	0.33	0.065	43.51	0.845	0.218	0.41
	0.41	0.073	65.96	0.991		
	0.52	0.084	85.66	1.162		
	0.81	0.107	96.49	1.303		
90% BW + 10% EVA	0.21	0.058	48.97	0.766	0.094	0.56
	0.25	0.066	70.46	0.904		
	0.28	0.070	87.37	1.011		
	0.38	0.088	95.84	1.118		
80% BW + 20% EVA	0.34	0.039	48.93	0.534	0.072	0.59
	0.42	0.050	68.71	0.671		
	0.58	0.059	88.71	0.779		
	0.64	0.070	95.06	0.907		
89% BW + 10% EVA + 1% AC	0.25	0.059	45.45	0.781	0.154	0.41
	0.43	0.068	71.08	0.935		
	0.52	0.071	84.73	1.043		
	0.79	0.90	91.19	1.132		
78% BW + 20% EVA + 2% AC	0.38	0.047	47.43	0.637	0.334	0.53
	0.42	0.056	69.41	0.747		
	0.57	0.064	87.09	0.842		
	0.59	0.074	97.91	0.957		

* Oxidizer mass flux uncertainty range: 1.4–4.7%. # Mass flux exponent (*n*) uncertainty range: 1.3–2.6%.

Table 4. Viscosity of BW–EVA-based solid fuels.

Fuel Sample	Viscosity (Cp) at 90 °C, 22 S^{-1}	Reduction in Regression Rate (%) *
100% BW	1.7	-
90% BW + 10% EVA	18.1	25
80% BW + 20% EVA	38.5	32
89% BW + 10% EVA + 1% AC	29.4	15
78% BW + 20% EVA + 2% AC	48.7	30

* Percentage reduction in regression rate at 95 kg/m^2-s relative to 100% BW.

Even though the regression rate increased when AC was added to BW–EVA blends, it was still lower than with pure BW. This could be because adding AC to the BW–EVA matrix increased the viscosity of the blend, as shown in Table 4. There was a significant difference between the viscosities of the tested fuels. As a result, both the regression rates and the droplet entrainment process during combustion were affected. From Figure 8, it can be seen that the B2 (90% BW + 10% EVA) and B3 (80% BW + 20% EVA) fuel samples exhibited lower regression rates compared to the B4 (89% BW + 10% EVA + 1% AC) and B5 (78% BW+20% EVA + 2% AC) samples (doped with AC). This regression rate enhancement can be ascribed to radiation heat transfer from the AC particles at the combustion zone to the surface of the high viscous fuel melt layer. Therefore, a careful trade-off must be made to obtain superior fuel composition when AC is added. However, in the context of the present study, it is recommended that less than 2% AC is used in BW–EVA compositions for better regression rates. Carmicino et al. [57] showed that the addition of 3 wt.% CB to HTPB fuel enhanced the regression rate up to 30%. Therefore, it would be interesting to study in detail the definite role of opacifiers (carbon black or AC) loading on the performance of solid fuels with different combustion behavior such as pure wax, wax polymer, and HTPB in hybrid rockets. The authors are currently investigating this aspect separately, and it will be highlighted in a future study.

One shortcoming of hybrid rockets is the oxidizer-to-fuel ratio (O/F) variation during the motor operation. The variation in the O/F ratio leads to a change in the characteristic velocity and specific impulse. The O/F ratio shift is generally quantified with the mass flux index (n). To counteract the O/F shift during burning, the mass flux index should be approximately equal to 0.5. Table 3 provides the mass flux index for each fuel composition investigated in the present study. It can be observed that the value of 'n' for most of the fuel compositions varies between 0.41 and 0.59, which suggests that there is a slight shift in the O/F ratio (for the B1–B4 samples) during the combustion process.

3.4. Combustion Efficiency Characterization

The chamber pressure is a critical parameter in determining combustion efficiency. During the lab-scale ballistic test, the chamber pressure was recorded with the burn time and is presented in Figure 9. The total combustion time used for the entire experiment was 5 s. The major events that occurred during the ballistic test firing were highlighted in the pressure–time curve. It is clear that after the injection of the oxidizer and ignition, it takes less than a second to attain the nominal combustion chamber pressure. After the combustion was quasi-steady, the solenoid valve cut off the oxidizer supply and consequently terminated the combustion. Figure 9 shows that BW–EVA has relatively stable combustion compared to pure BW-based fuel. This could be due to entrained liquid fuel droplets from the burning fuel surface and periodic oscillations in the liquid layer. With the BW–EVA sample, the combustion is smooth over a range of burn times and could be attributed to improved wax melt layer thermal stability due to increased viscosity. As explained earlier, with an increase in the melt layer, the pyrolyzed fuel is transported to the flame zone in vapor form instead of droplets. These fuel vapors mix with oxygen easily and combust efficiently as compared to droplets. Therefore, smooth combustion was observed with BW–EVA fuel compositions. The pressure fluctuation observed with a pure

BW sample is relatively small and does not affect the operation of the hybrid rocket motor. The chamber pressure data for all the tested fuel formulations are presented in Table 3.

The combustion efficiency based on the characteristic velocity of the BW–EVA/AC fuel compositions has been determined through ballistic tests. The theoretical characteristic velocity was calculated using the NASA CEA code [53]. The experimental characteristic velocity was evaluated based on experimental conditions, as explained in Section 2.5. Figure 10 shows the variation of theoretical and experimental characteristic velocities for different O/F ratios.

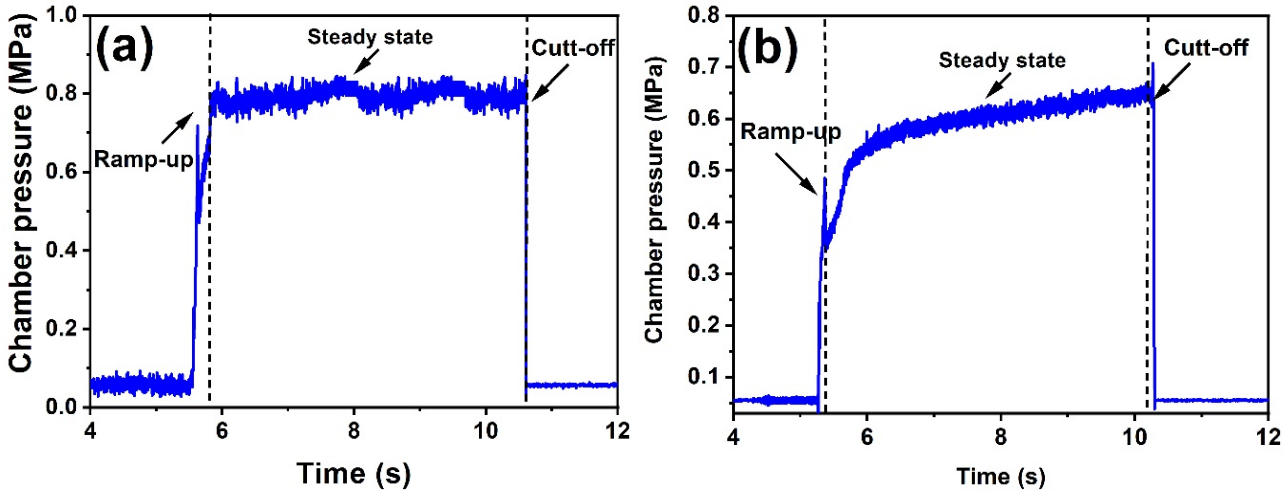

Figure 9. Combustion chamber pressure of (**a**) pure beeswax and (**b**) 80% beeswax + 20% EVA.

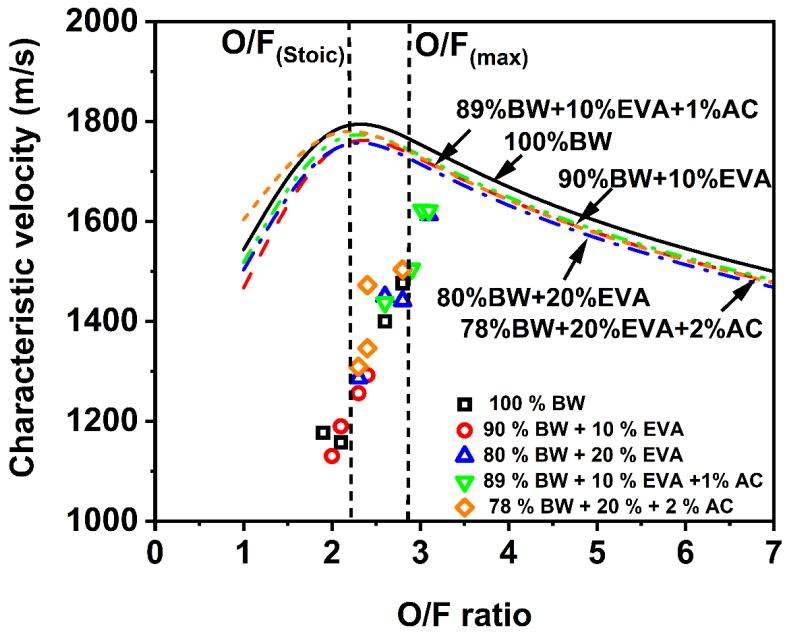

Figure 10. Characteristic velocity variation vs. O/F ratio for prepared fuels (lines and symbols are theoretical and experimental values, respectively).

It can be seen that the maximum characteristic velocity resides between 2 and 2.5 $(O/F)_{max}$, whereas the stochiometric O/F ratios are found to be in the range of 2.2 to 2.8. The characteristic velocity is found to decrease with the addition of EVA, which could be due to the reduced wt.% of the wax in the fuel matrix compared to pure BW. The combustion efficiencies of BW-based fuel were calculated using the experimental and theoretical characteristic velocity and are presented in Figure 11.

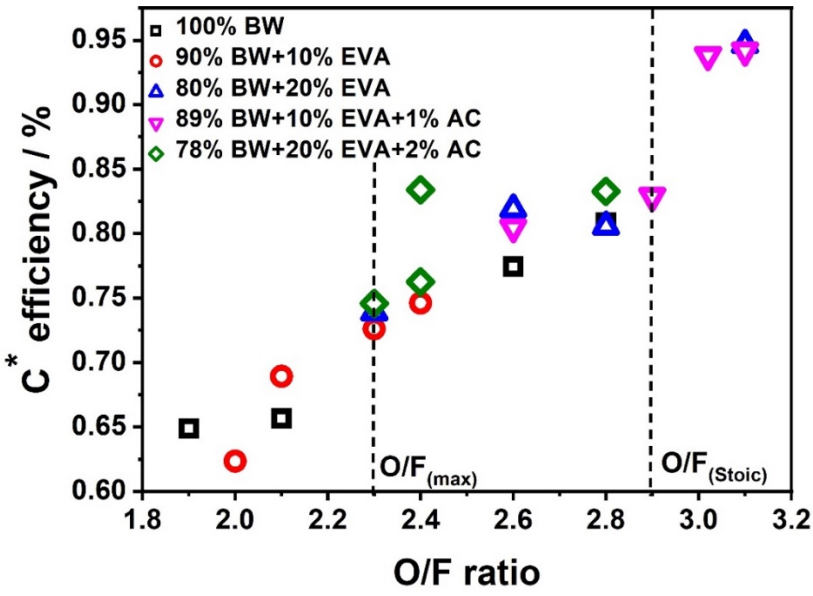

Figure 11. Combustion efficiency variation vs. O/F ratio for prepared fuels.

The combustion efficiency of tested fuel compositions is found to be in the range of 62% to 94%. The combustion efficiency of BW-based fuel is improved when the hybrid motor is operated close to $(O/F)_{stoic}$. In general, the combustion efficiency can be augmented by increasing the characteristic length (L*), oxidizer mass flux, and $(O/F)_{stoic}$ [37,38]. Figure 11 shows that the pure BW exhibited poor combustion efficiency for the corresponding O/F ratios. One of the drawbacks of using pure wax fuels is their generally poor combustion efficiency. The reason for poor combustion efficiency is the entrainment of fuel droplets and the diffusion-limited combustion process in hybrid rockets. Kim et al. [30] conducted lab-scale combustion experiments to elucidate the poor combustion efficiency of wax fuels. It was reported that incomplete combustion occurred due to the limited combustion time scale of the droplets within the chamber. As a result, the unburnt fuel droplets leave the combustion chamber as unutilized fuel products, leading to lower combustion efficiency.

Furthermore, it was observed that the combustion efficiency was improved by adding EVA to BW. Table 4 also shows that the fuels blended with EVA have a higher viscosity than the BW-based fuels. If the viscosity is higher, it is feasible that the droplets will not be able to entrain from the viscous melt layer; instead, the thick melt layer generates a large amount of fuel vapor through pyrolysis similar to conventional hybrid rocket combustion [32,34]. However, in the case of BW–EVA, the pyrolysis was much faster; hence, it produced a higher regression rate. The fuel vapors could mix easily with the available gaseous oxygen and combust completely. Thus, higher combustion efficiency was observed with EVA blended fuels than with pure BW. The combustion efficiency was observed to be increased with the addition of 2% AC to the BW-20% EVA composition at 2.8 O/F. It can be seen from Table 4 B5 fuel sample has a higher viscosity, which might have led to an increase in combustion efficiency. However, there is no correlation in the literature to predict the combustion efficiency based on the viscosity of the melt layer; for regression rates, see references [32–34]. It was understood from this study that when blending wax fuels with polymeric additives, a reasonable balance should be established between regression rate, combustion efficiency, and mechanical properties.

4. Conclusions

The current study examined the thermal and ballistic properties of solid fuels derived from BW and blended with EVA/AC. Thermal stability and surface morphological observation were assessed using TGA and SEM analytical instruments. The ballistic characterization was carried out using a laboratory-scale hybrid rocket. Key performance

parameters such as regression rate and combustion efficiency of BW-based fuel were evaluated. The following conclusions were drawn from the thermal and ballistic test results:

- The thermal stability of BW-based fuel was improved with the addition of EVA. The onset decomposition temperature increased from 205 °C to 227.3 °C when 20 wt.% EVA was added to BW.
- The thermal decomposition of BW–EVA samples was improved with the addition of AC. However, a marginal reduction in thermal stability was observed for the BW–EVA/AC-based fuel, which positively affected the regression rate performance.
- The viscosity of BW-based fuel formulations was increased significantly when EVA and AC were added to the BW matrix. The viscosity for pure BW was found to be 1.7 cp, which increased to 38.5 cp with the addition of EVA.
- Ballistic tests revealed that the pure BW displayed the highest regression rate among tested fuel formulations. The regression rate was reduced by adding EVA to BW matrix, which was attributed to the increased viscosity of the liquid melt layer. Furthermore, the regression rate was improved by adding AC to BW–EVA fuels.
- The combustion efficiency of BW-based fuel was improved from 62% to 94% when 20 wt.% of EVA and 2 wt.% of AC were added to BW fuel.

Author Contributions: Funding acquisition, S.N.M.; Investigation, S.N.M., Y.P., M.D. and A.I. All authors have read and agreed to the published version of the manuscript.

Funding: This research received no external funding.

Data Availability Statement: Data available on request from the authors.

Acknowledgments: We express our sincere thanks to the SAIF facility, IIT Madras, for providing access to the facility to conduct TG-DSC experiments. We are also thankful to SAIF Cochin University for helping to conduct SEM analysis.

Conflicts of Interest: The authors declare no conflict of interest.

References

1. Mazzetti, A.; Merotto, L.; Pinarello, G. Paraffin-Based Hybrid Rocket Engines Applications: A Review and a Market Perspective. *Acta Astronaut.* **2016**, *126*, 286–297. [CrossRef]
2. Mahottamananda, S.N.; Kadiresh, N.P.; Pal, Y. Regression Rate Characterization of HTPB-Paraffin Based Solid Fuels for Hybrid Rocket. *Propellants Explos. Pyrotech.* **2020**, *45*, 1755–1763. [CrossRef]
3. Chiaverini, M.J. Review of Solid-Fuel Regression Rate Behavior in Classical and Nonclassical Hybrid Rocket Motors. In *Fundamentals of Hybrid Rocket Combustion and Propulsion*; Kuo, K.K., Chiaverini, M.J., Eds.; American Institute of Aeronautics and Astronautics: Reston, VA, USA, 2007; pp. 37–126. ISBN 978-1-56347-703-4.
4. Mukunda, H.S.; Jain, V.K.; Paul, P.J. A Review of Hybrid Rockets: Present Status and Future Potential. *Proc. Indian Acad. Sci. Sect. C Eng. Sci.* **1979**, *2*, 215–242. [CrossRef]
5. Pal, Y.; Mahottamananda, S.N.; Palateerdham, S.K.; Subha, S.; Ingenito, A. Review on the Regression Rate-Improvement Techniques and Mechanical Performance of Hybrid Rocket Fuels. *FirePhysChem* **2021**, *1*, 272–282. [CrossRef]
6. Mahottamananda, S.N.; Kadiresh, P.N.; Pal, Y. A Study on Thermal Stability and Combustion Performance of Hydroxyl-Terminated Polybutadiene-Paraffin Blended Fuel. *Energy Sources Part A Recovery Util. Environ. Eff.* **2020**. [CrossRef]
7. Natan, B.; Gany, A. Combustion Characteristics of a Boron-Fueled Solid Fuel Ramjet with Aft-Burner. *J. Propuls. Power* **1993**, *9*, 694–701. [CrossRef]
8. Metals, Energetic Additives, and Special Binders Used in Solid Fuels for Hybrid Rockets. In *Fundamentals of Hybrid Rocket Combustion and Propulsion*; Progress in Astronautics and Aeronautics; American Institute of Aeronautics and Astronautics: Reston, VA, USA, 2007; pp. 413–456. ISBN 978-1-56347-703-4.
9. Larson, D.; Boyer, E.; Wachs, T.; Kuo, K.; DeSain, J.; Curtiss, T.; Brady, B. Characterization of the Performance of Paraffin/LiAlH4 Solid Fuels in a Hybrid Rocket System. In Proceedings of the 47th AIAA/ASME/SAE/ASEE Joint Propulsion Conference & Exhibit, San Diego, CA, USA, 31 July–3 August 2011; American Institute of Aeronautics and Astronautics: Reston, VA, USA, 2022.
10. Boiocchi, M.; Maggi, F.; Paravan, C.; Galfetti, L. Paraffin-Based Fuels and Energetic Additives for Hybrid Rocket Propulsion. In Proceedings of the 51st AIAA/SAE/ASEE Joint Propulsion Conference, Orlando, FL, USA, 27–29 July 2015; AIAA Propulsion and Energy Forum. American Institute of Aeronautics and Astronautics: Reston, VA, USA, 2015.
11. Galfetti, L.; Merotto, L.; Boiocchi, M.; Maggi, F.; DeLuca, L.T. Experimental Investigation of Paraffin-Based Fuels for Hybrid Rocket Propulsion. *Prog. Propuls. Phys.* **2013**, *4*, 59–74.

12. Kim, S.; Kim, J.; Moon, H.; Sung, H.; Lee, J.; Kim, G.; Cho, J.; Park, S. Combustion Characteristics of the Cylindrical Multi-Port Grain for Hybrid Rocket Motor. In Proceedings of the 45th AIAA/ASME/SAE/ASEE Joint Propulsion Conference & Exhibit, Denver, CO, USA, 2–5 August 2009; ISBN 978-1-60086-972-3.
13. Tian, H.; Li, X.; Peng, Z.; Yu, N.; Cai, G. Numerical and Experimental Studies of the Hybrid Rocket Motor with Multi-Port Fuel Grain. *Acta Astronaut.* **2014**, *96*, 261–268. [CrossRef]
14. George, P.; Krishnan, S.; Varkey, P.M.; Ravindran, M.; Ramachandran, L. Fuel Regression Rate in Hydroxyl-Terminated-Polybutadiene/Gaseous-Oxygen Hybrid Rocket Motors. *J. Propuls. Power* **2001**, *17*, 35–42. [CrossRef]
15. Frederick, R.A.; Whitehead, J.J.; Knox, L.R.; Moser, M.D. Regression Rates Study of Mixed Hybrid Propellants. *J. Propuls. Power* **2007**, *23*, 175–180. [CrossRef]
16. Karabeyoglu, M.; Cantwell, B.; Altman, D. Development and Testing of Paraffin-Based Hybrid Rocket Fuels. In Proceedings of the 37th Joint Propulsion Conference and Exhibit, Salt Lake, UT, USA, 8–11 July 2001; American Institute of Aeronautics and Astronautics: Reston, VA, USA, 2001.
17. Heydari, M.M.; Ghadiri Massoom, N. Experimental Study of the Swirling Oxidizer Flow in HTPB/N_2O Hybrid Rocket Motor. *Int. J. Aerosp. Eng.* **2017**, *2017*, 3174140. [CrossRef]
18. Kumar, C.P.; Kumar, A. Effect of Swirl on the Regression Rate in Hybrid Rocket Motors. *Aerosp. Sci. Technol.* **2013**, *29*, 92–99. [CrossRef]
19. Chidambaram, P.K.; Kumar, A. Effect of Diaphragms on Regression Rate in Hybrid Rocket Motors. *J. Propuls. Power* **2013**, *29*, 559–572. [CrossRef]
20. Kumar, R.; Ramakrishna, P.A. Effect of Protrusion on the Enhancement of Regression Rate. *Aerosp. Sci. Technol.* **2014**, *39*, 169–178. [CrossRef]
21. Dinesh, M.; Rajput, S.S.; Kumar, R. Protrusion Effect on the Performance of Hybrid Rocket with Liquefying and Non-Liquefying Fuels. *Acta Astronaut.* **2021**, *178*, 536–547. [CrossRef]
22. Dinesh, M.; Kumar, R. Utility of Multiprotrusion as the Performance Enhancer in Hybrid Rocket Motor. *J. Propuls. Power* **2019**, *35*, 1005–1017. [CrossRef]
23. Dinesh, M.; Kumar, R. Effect of Protrusion on Combustion Stability of Hybrid Rocket Motor. *Propellants Explos. Pyrotech.* **2022**, *47*, e202100067. [CrossRef]
24. Dinesh, M.; Kumar, R. Experimental Studies of Protrusion-Inserted Hybrid Rocket Motor with Varying L/D Ratio. *J. Spacecr. Rocket.* **2021**, *58*, 134–147. [CrossRef]
25. Kumar, R.; Periyapatna, R. Enhancement of Hybrid Fuel Regression Rate Using a Bluff Body. *J. Propuls. Power* **2014**, *30*, 909–916. [CrossRef]
26. Wu, Y.; Yu, X.; Lin, X.; Li, S.; Wei, X.; Zhu, C.; Wu, L. Experimental Investigation of Fuel Composition and Mix-Enhancer Effects on the Performance of Paraffin-Based Hybrid Rocket Motors. *Aerosp. Sci. Technol.* **2018**, *82*, 620–627. [CrossRef]
27. Cai, G.; Cao, B.; Zhu, H.; Tian, H.; Ma, X. Parametric Investigation of Secondary Injection in Post-Chamber on Combustion Performance for Hybrid Rocket Motor. *Acta Astronaut.* **2017**, *140*, 427–438. [CrossRef]
28. Sinha, Y.K.; Sridhar, B.T.N.; Kishnakumar, R. Study of Thermo-Mechanical Properties of HTPB–Paraffin Solid Fuel. *Arab. J. Sci. Eng.* **2016**, *41*, 4683–4690. [CrossRef]
29. Jayapal, S.N.M.; Dubey, V.K.; Dinesh, S.; Wahab, A.; Abdul Khaleel, A.; Kadiresh, P.N. Thermal Stability and Kinetic Study of Blended Beeswax-Ethylene Vinyl Acetate Based Hybrid Rocket Fuels. *Thermochim. Acta* **2021**, *702*, 178989. [CrossRef]
30. Kim, S.; Moon, H.; Kim, J. Thermal Characterizations of the Paraffin Wax/Low Density Polyethylene Blends as a Solid Fuel. *Thermochim. Acta* **2015**, *613*, 9–16. [CrossRef]
31. Pal, Y.; Kumar, V.R. Thermal Decomposition Study of Paraffin Based Hybrid Rocket Fuel Containing Aluminum and Boron Additives. *Thermochim. Acta* **2017**, *655*, 63–75. [CrossRef]
32. Tang, Y.; Chen, S.; Zhang, W.; Ruiqi, S.; DeLuca, L.; Ye, Y. Mechanical Modifications of Paraffin-Based Fuels and the Effects on Combustion Performance. *Propellants Explos. Pyrotech.* **2017**, *42*, 1268–1277. [CrossRef]
33. Kim, S.; Moon, H.; Kim, J.; Cho, J. Evaluation of Paraffin–Polyethylene Blends as Novel Solid Fuel for Hybrid Rockets. *J. Propuls. Power* **2015**, *31*, 1750–1760. [CrossRef]
34. Kobald, M.; Schmierer, C.; Ciezki, H.; Schlechtriem, S.; Toson, E.; DeLuca, L. Viscosity and Regression Rate of Liquefying Hybrid Rocket Fuels. *J. Propuls. Power* **2017**, *33*, 1245–1251. [CrossRef]
35. Veale, K.; Adali, S.; Pitot, J.; Brooks, M. A Review of the Performance and Structural Considerations of Paraffin Wax Hybrid Rocket Fuels with Additives. *Acta Astronaut.* **2017**, *141*, 196–208. [CrossRef]
36. Nakagawa, I.; Nikone, S. Study on the Regression Rate of Paraffin-Based Hybrid Rocket Fuels. *J. Propuls. Power* **2011**, *27*, 1276–1279. [CrossRef]
37. Karabeyoglu, M.A.; Altman, D.; Cantwell, B.J. Combustion of Liquefying Hybrid Propellants: Part 1, General Theory. *J. Propuls. Power* **2002**, *18*, 610–620. [CrossRef]
38. Karabeyoglu, M.A.; Cantwell, B.J. Combustion of Liquefying Hybrid Propellants: Part 2, Stability of Liquid Films. *J. Propuls. Power* **2002**, *18*, 621–630. [CrossRef]
39. Pal, Y.; Kumar, K.H.; Li, Y.-H. Ballistic and Mechanical Characteristics of Paraffin-Based Solid Fuels. *CEAS Space J.* **2019**, *11*, 317–327. [CrossRef]
40. Kumar, R.; Ramakrishna, P.A. Studies on EVA-Based Wax Fuel for Launch Vehicle Applications. *Propellants Explos. Pyrotech.* **2016**, *41*, 295–303. [CrossRef]

41. Evans, B.; Boye, E.; Kuo, K.; Risha, G.; Chiaverini, M. Hybrid Rocket Investigation at Penn State University's High-Pressure Combustion Laboratory: Overview and Recent Results. In Proceedings of the 45th AIAA/ASME/SAE/ASEE Joint Propulsion Conference and Exhibit, Denver, CO, USA, 2–5 August 2009. AIAA Paper 2009-5349.
42. Hashim, S.A.; Islam, M.; Kangle, S.M.; Karmakar, S.; Roy, A. Performance Evaluation of Boron/Hydroxyl-Terminated Polybutadiene-Based Solid Fuels Containing Activated Charcoal. *J. Spacecr. Rocket.* **2021**, *58*, 363–374. [CrossRef]
43. Verma, S.; Periyapatna, R. Investigations on Activated Charcoal, a Burn-Rate Enhancer in Composite Solid Propellant. *J. Propuls. Power* **2013**, *29*, 1214–1219. [CrossRef]
44. Putnam, S.G. Investigation of Non-Conventional Bio-Derived Fuels for Hybrid Rocket Motors. Ph.D. Thesis, The University of Tennessee, Knoxville, TN, USA, 2017; 145p.
45. Scholes, J. Bio-Derived Fuels for Hybrid Rocket Motors. Master's Thesis, University of Tennessee, Knoxville, TN, USA, 2005.
46. Makled, E.-S.M. Beeswax Material: Non-Conventional Solid Fuel for Hybrid Rocket Motors. *Adv. Mil. Technol.* **2019**, *14*, 99–113. [CrossRef]
47. Stober, K.J.; Sanchez, A.; Wanyiri, J.; Jiwani, S.; Wood, D. Centrifugal Casting of Paraffin and Beeswax for Hybrid Rockets. In Proceedings of the AIAA Propulsion and Energy 2020 Forum, Virtual Event, 24–28 August 2020; American Institute of Aeronautics and Astronautics: Reston, VA, USA, 2020.
48. Naoumov, V.; Al-Masoud, N.; Butt, J.; Correa, C.; Parmelee, D.; Couillard, M.; Nguyen, H.; Ampofo, J.; Patel, K. Student-Faculty Research on the Combustion of Non-Conventional Fuels in Hybrid Propellant Rocket Engine in a Wide Range of Oxidizer-to-Fuel Ratios. In Proceedings of the AIAA SciTech 2020 Forum, Orlando, FL, USA, 6–10 January 2020. [CrossRef]
49. Dubey, V.K.; Mahottamananda, S.N.; Khaleel, A.A.; Kadiresh, P.N.; Thirumurugan, M. Mechanical Characteristics of Paraffin Wax, Beeswax and HTPB as Rocket Propellant—A Comparative Study. In *Advances in Design and Thermal Systems*; Ganippa, L., Karthikeyan, R., Muralidharan, V., Eds.; Springer: Singapore, 2021; pp. 243–252. [CrossRef]
50. Sri Nithya Mahottamananda, J.; Vanchhit Kumar, D.; Afreen, A.K.; Dinesh, S.; Ashiq, W.; Kadiresh, P.N.; Thirumurugan, M. Mechanical Characteristics of Ethylene Vinyl Acetate Mixed Beeswax Fuel for Hybrid Rockets. In *Advances in Design and Thermal Systems*; Ganippa, L., Karthikeyan, R., Muralidharan, V., Eds.; Lecture Notes in Mechanical Engineering; Springer: Singapore, 2021. [CrossRef]
51. Kumar, R.; Ramakrishna, P.A. Issues Related to the Measurement of Regression Rate of Fast-Burning Hybrid Fuels. *J. Propuls. Power* **2013**, *29*, 1114–1121. [CrossRef]
52. Paul, P.J.; Mukunda, H.S.; Narahari, H.K.; Venkataraman, R.; Jain, V.K. Regression Rate Studies in Hypergolic System. *Combust. Sci. Technol.* **1981**, *26*, 17–24. [CrossRef]
53. Gordon, S.; Mcbride, B.J. *Computer Program for Calculation of Complex Chemical Equilibrium Compositions and Applications. Part 1: Analysis*; NASA: Washington, DC, USA, 1994; pp. 1–61.
54. Buchwald, R.; Breed, M.D.; Greenberg, A.R. The Thermal Properties of Beeswaxes: Unexpected Findings. *J. Exp. Biol.* **2008**, *211*, 121–127. [CrossRef]
55. DeSain, J.; Brady, B.; Metzler, K.; Curtiss, T.; Albright, T. Tensile Tests of Paraffin Wax for Hybrid Rocket Fuel Grains. In Proceedings of the 45th AIAA/ASME/SAE/ASEE Joint Propulsion Conference & Exhibit; Joint Propulsion Conferences, Denver, CO, USA, 2–5 August 2009; American Institute of Aeronautics and Astronautics: Reston, VA, USA, 2009.
56. Mengu, D.; Kumar, R. Development of EVA-SEBS Based Wax Fuel for Hybrid Rocket Applications. *Acta Astronaut.* **2018**, *152*, 325–334. [CrossRef]
57. Carmicino, C.; Scaramuzzino, F.; Russo Sorge, A. Trade-off between Paraffin-Based and Aluminium-Loaded HTPB Fuels to Improve Performance of Hybrid Rocket Fed with N_2O. *Aerosp. Sci. Technol.* **2014**, *37*, 81–92. [CrossRef]